Experimental Gerontology 103 (2018) 35–46

Contents lists available at ScienceDirect

Experimental Gerontology

journal homepage: www.elsevier.com/locate/expgero

# The impact of mechanically stimulated muscle-derived stromal cells on aged skeletal muscle

Heather D. Huntsman[a,b], Catarina Rendeiro[b,c,1], Jennifer R. Merritt[b,d], Yair Pincu[a,b], Adam Cobert[b,d], Michael De Lisio[a,b], Emily Kolyvas[b], Svyatoslav Dvoretskiy[a,b], Iwona T. Dobrucki[b], Ralf Kemkemer[e], Tor Jensen[f], Lawrence W. Dobrucki[b,g], Justin S. Rhodes[b,c,d], Marni D. Boppart[a,b,c,*]

[a] Department of Kinesiology and Community Health, University of Illinois at Urbana-Champaign, Urbana, IL 61801, USA
[b] Beckman Institute for Advanced Science and Technology, University of Illinois at Urbana-Champaign, Urbana, IL 61801, USA
[c] Center for Nutrition, Learning and Memory, University of Illinois at Urbana-Champaign, Urbana, IL 61801, USA
[d] Department of Psychology and Neuroscience Program, University of Illinois at Urbana-Champaign, Urbana, IL 61801, USA
[e] Department of New Materials and Biosystems, Max Planck Institute for Intelligent Systems, Stuttgart, Germany
[f] Division of Biomedical Sciences, Carle Hospital, Urbana, IL 61801, USA
[g] Department of Bioengineering, University of Illinois at Urbana-Champaign, Urbana, IL 61801, USA

ARTICLE INFO

Editor: Christiaan Leeuwenburgh

*Keywords:*
Aging
Skeletal muscle
Perivascular stromal cells
Mesenchymal stem cells
Exercise
Vascular perfusion
Neurogenesis
Cognition

ABSTRACT

Perivascular stromal cells, including mesenchymal stem/stromal cells (MSCs), secrete paracrine factor in response to exercise training that can facilitate improvements in muscle remodeling. This study was designed to test the capacity for muscle-resident MSCs (mMSCs) isolated from young mice to release regenerative proteins in response to mechanical strain *in vitro*, and subsequently determine the extent to which strain-stimulated mMSCs can enhance skeletal muscle and cognitive performance in a mouse model of uncomplicated aging. Protein arrays confirmed a robust increase in protein release at 24 h following an acute bout of mechanical strain *in vitro* (10%, 1 Hz, 5 h) compared to non-strain controls. Aged (24 month old), C57BL/6 mice were provided bilateral intramuscular injection of saline, non-strain control mMSCs, or mMSCs subjected to a single bout of mechanical strain *in vitro* ($4 \times 10^4$). No significant changes were observed in muscle weight, myofiber size, maximal force, or satellite cell quantity at 1 or 4 wks between groups. Peripheral perfusion was significantly increased in muscle at 4 wks post-mMSC injection ($p < 0.05$), yet no difference was noted between control and preconditioned mMSCs. Intramuscular injection of preconditioned mMSCs increased the number of new neurons and astrocytes in the dentate gyrus of the hippocampus compared to both control groups ($p < 0.05$), with a trend toward an increase in water maze performance noted ($p = 0.07$). Results from this study demonstrate that acute injection of exogenously stimulated muscle-resident stromal cells do not robustly impact aged muscle structure and function, yet increase the survival of new neurons in the hippocampus.

## 1. Introduction

Mesenchymal stem/stromal cells (MSCs) reside in close proximity to vessels in nearly all tissues, directly replacing injured tissue or indirectly facilitating repair and remodeling *via* secretion of growth factors and other small regenerative molecules [Augello et al., 2010; Meirelles Lda et al., 2009; Murray et al., 2014]. We recently demonstrated that perivascular, muscle-resident MSCs (mMSCs), isolated based on positive selection for stem cell antigen-1 (Sca-1) and negative selection for the hematopoietic cell marker CD45, can promote Pax7$^+$ progenitor cell (satellite cell) quantity, new fiber formation, myonuclear accumulation, arteriogenesis, and myofiber size when injected into skeletal muscle immediately prior to an eccentric exercise training program in a mouse model [Huntsman et al., 2013; Valero et al., 2012; Zou et al., 2015]. Transplantation in the absence of exercise training did not confer any benefit, highlighting the importance of mechanical strain or a similar exercise-specific cue in mMSC-mediated skeletal muscle adaptation [Huntsman et al., 2013; Valero et al., 2012; Zou et al., 2015]. Our prior studies also demonstrate that mMSCs are non-myogenic, as mMSCs do not form myotubes in culture and do not

* Corresponding author at: Beckman Institute for Advanced Science and Technology, 405 N. Mathews Avenue, MC-251, Urbana, IL 61801, USA.
*E-mail addresses:* C.Rendeiro@bham.ac.uk (C. Rendeiro), mboppart@illinois.edu (M.D. Boppart).
[1] Current address: School of Sport, Exercise and Rehabilitation Sciences, University of Birmingham, Birmingham, UK B15 2TT.

https://doi.org/10.1016/j.exger.2017.12.012
Received 30 August 2017; Received in revised form 16 November 2017; Accepted 14 December 2017
Available online 18 December 2017
0531-5565/ 

directly fuse with muscle fibers *in vivo* [Valero et al., 2012; Zou et al., 2015]. Thus, perivascular stromal cells contribute to exercise-induced structural and functional gains in a manner that does not require myogenesis.

Aging can significantly reduce the potential for skeletal muscle to grow in response to anabolic stimuli, including exercise and/or amino acid consumption in humans and mice [Katsanos et al., 2006; Kumar et al., 2009; Lee et al., 2016]. The molecular basis for anabolic resistance and subsequent declines in mass and function is controversial, yet inadequate progenitor cell activation and muscle protein turnover likely contribute [Carnio et al., 2014; Conboy et al., 2003; Fan et al., 2016]. Perivascular stromal cells, including mMSCs, may also underlie anabolic resistance in the context of aging. We recently isolated and evaluated perivascular stromal cell function in sedentary (non-exercised) aged mice compared to young adult controls [Munroe et al., 2017]. The results from this study demonstrated that mMSC gene expression is robustly compromised in aged muscle, as evidenced by reduced transcription of several regenerative growth [epidermal growth factor (EGF), leukemia inhibitory factor (LIF), hepatocyte growth factor (HGF), insulin-like growth factor 1 (IGF-1), vascular endothelial growth factor alpha (VEGFα)], neurotrophic [brain-derived neurotrophic factor (BDNF), nerve growth factor (NGF), fibronectin type II domain 5 (Fndc5)], and ECM remodeling proteins [matrix metalloproteinases 2 and 14 (MMP2/14), collagen 1α1] that are collectively important for muscle repair and remodeling. Tumor necrosis alpha (TNFα) gene expression was also elevated in aged mMSCs compared to young. The aged mMSC transcriptional signature suggests that aberrant stromal cell function may contribute to anabolic resistance and the subsequent loss of muscle structure and function during the natural process of aging [Munroe et al., 2017]. This information, as well as the unique immune-privileged status of MSCs [Meirelles Lda et al., 2009; Ranganath et al., 2012] and limitations associated with satellite cell transplantation, justify the development of mMSC-focused strategies for the prevention and treatment of age-related disability.

A majority of older adults possess some capacity to exercise, and engagement in a physical activity program may be sufficient to maintain mMSC function and strength throughout the lifespan. However, disability can occur with extended bedrest due to disease or injury, and an alternative cell-based therapy may be desirable. One of the challenges of creating a stromal cell-based therapy is the requirement of promoting stimulation and release of regenerative factors upon transplantation. Our *in vitro* experiments to date have demonstrated specific sensitivity of mMSCs to force, as a single bout of mechanical strain (10% biaxial, 1 Hz, 5 h) can significantly enhance the capacity for freshly isolated mMSCs to secrete EGF (4-fold), granulocyte macrophage colony-stimulating factor (GM-CSF) (3-fold), and HGF (1.5-fold), among other proteins [Huntsman et al., 2013]. The full data set from our protein array is now reported. Based on the results, we speculated that mechanical strain preconditioning of mMSCs prior to transplantation could potentially promote the release of regenerative factors necessary to initiate adaptation in aged skeletal muscle in the absence of exercise, including progenitor cell activation and myofiber growth. In addition, consistent with 1) recent studies that suggest a role for systemic factors in exercise-mediated neuroplasticity [Gu et al., 2012; Moon et al., 2016; Wrann et al., 2013] and 2) evidence of a decline in mMSC neurogenic factor secretion (BDNF, NGF, FNDC5) in aged muscle [Munroe et al., 2017], we secondarily hypothesized that intramuscular transplantation of preconditioned mMSCs could confer beneficial outcomes in the distal central nervous system.

Here we report that a single intramuscular injection of young mMSCs preconditioned with mechanical strain did not robustly initiate skeletal muscle adaptation in the absence of overt injury and disease, yet significantly increased the quantity of new neurons in the hippocampus of aged mice.

## 2. Methods

### 2.1. Animals

Protocols for animal use were reviewed and approved by the Institutional Animal Care and Use Committee (IACUC) of the University of Illinois at Urbana-Champaign. Animals were fed standard laboratory chow and had access to water *ad libitum*. Mice were housed in a temperature-controlled specific pathogen-free animal room maintained on a 12:12 light-dark cycle at the animal facility at the Beckman Institute. Five wk. old C57BL/6 mice were used for all mMSC isolation and transplantation experiments. Aged mice (C57BL/6, 24 months, female) were acquired from National Institute of Aging (NIA) colonies and used as recipients for mMSC transplantation. Mice were acclimated to the housing room for at least 1 wk prior to each experiment.

### 2.2. Isolation of MSCs from skeletal muscle (mMSCs)

Five wk. old C57BL/6 mice were subjected to a single bout of eccentric exercise (−20° treadmill run, 17 m/min, 30 min) prior to isolation of stem cells to increase yield necessary for transplantation. At 24 h post-exercise, gastrocnemius-soleus complexes were excised and Sca-1$^+$CD45$^-$ cells were isolated as previously reported [Huntsman et al., 2013]. Briefly, after mechanical disruption and enzymatic digestion of the dissected muscle tissue, filtered samples were incubated in anti-mouse CD16/CD32 (1 μg/10$^6$ cells) (eBioscience, San Diego, CA) to block non-specific Fc-mediated interactions and then stained in a cocktail of monoclonal anti-mouse antibodies Sca-1-PE (600 ng/10$^6$ cells) and CD45-APC (300 ng/10$^6$ cells) (eBioscience) diluted in 2% FBS in phosphate buffered saline (PBS). Fluorescence activated cell sorting (FACS) was performed using an iCyt Reflection System (Champaign, IL), located at Carle Hospital (Urbana, IL). Sca-1$^+$CD45$^-$ cells were collected in uncoated tissue culture dishes in medium incubated at 37 °C and 5% $CO_2$ for 8 to 10 days to allow for recovery and short-term expansion up to 80–90% confluency.

### 2.3. mMSC preconditioning

FACS recovered, unpassaged Sca-1$^+$CD45$^-$ cells were seeded at subconfluent levels onto pre-manufactured laminin peptide (YIGSR)-coated flexible silicone elastomer membrane plates (9.62 cm$^2$) at $1.0 \times 10^5$ cells/well ($10.4 \times 10^3$ cells/cm$^2$) (Flexcell International, McKeesport, PA). Cells were incubated in high glucose DMEM with 10% fetal bovine serum (FBS) at 37 °C and 5% $CO_2$ for 24 h to allow for sufficient cell attachment. Prior to mechanical strain, cells were washed with warm PBS and switched to serum-free high glucose DMEM. Equibiaxial mechanical strain (10%, 1 Hz) was applied to the cells for 5 h using a FX-4000 Flexercell strain unit (Flexcell International, McKeesport, PA). Cells maintained under static conditions were used as non-strained controls. Three hours following the completion of mechanical strain, cells were detached using an accutase enzyme solution and placed on gel elastomers for evaluation of gene expression *in vitro* or prepared for *in vivo* transplantation experiments (see sections below). In a separate experiment, conditioned media was collected 24 h following initiation of mechanical strain and analyzed with Proteome Profiler Antibody Arrays (ARY015, ARY013; R&D Systems, Minneapolis, MN) as previously described [Huntsman et al., 2013].

### 2.4. Evaluation of mMSC function on PDMS elastomer gels

To determine the extent to which mMSCs could sustain paracrine factor synthesis in a stiff, collagen-enriched microenvironment that replicated aged muscle, unstrained and strained mMSCs were placed on collagen-coated PDMS elastomer gels of varying stiffness for 1 wk prior to evaluation of gene expression. To create the gels, PDMS reagents (Dow Corning, Midland, MI) were mixed at ratios of 50:1, 40:1, and

20:1 base to curing agent, resulting in Young's elastic moduli (E) of 11 kPa, 30 kPa, and 110 kPa, respectively. Using 6-well tissue culture petri dishes, elastomers were poured to a thickness of 500 μm. Following a 15 min degassing period, gels were cured at 65 °C for 3 h. Elastomers were coated with Type I collagen (BD Biosciences, San Jose, CA). Following a 60 min incubation with collagen suspended in PBS at 100 μg/mL, the gels were washed with PBS and a 2% glutaraldehyde solution was added for 15 min to covalently link the protein to the PDMS elastomer. The elastomers were sterilized with 70% ethanol for 60 min. Each incubation period was carried out at room temperature. Gels were incubated overnight at 4 °C in a solution of 2 mM glycine to quench any excess aldehyde groups. Equal numbers ($2.5 \times 10^4$ cells/well) of non-strained and strained mMSCs were seeded onto PDMS gels. On Day 7, all cells were detached and live cells were counted using trypan blue staining. Following assessment of quantity, total RNA was extracted using the RNeasy Micro Kit and QIAshredder spin columns according to the manufacturer's specifications (Qiagen, Valencia, CA). The reverse transcriptase reaction was performed using a first strand cDNA synthesis kit (Applied Biosystems, Grand Island, NY). For detection of select genes (Taqman Primers: Egf Mm00438696, Hgf Mm01135193, Vegfa Mm01281449), cDNA was preamplified using TaqMan PreAmp Master Mix (Life Technologies Inc., Grand Island, NY). qPCR was completed and analyzed using the ΔΔCT method.

### 2.5. mMSC transplantation

Following mechanical strain preconditioning *in vitro*, mMSCs ($4 \times 10^4$ cells/50 μL HBSS per limb) were bilaterally administered to gastrocnemius-soleus muscle complexes of 24 month old, female WT mice while under anesthesia (1–3% isoflurane gas). Similar volumes of HBSS and unstrained mMSCs were injected into hindlimbs of separate mice to serve as controls. Mice were acquired and evaluated in four cohorts, with cohort 1 focusing on muscle and brain stem cell behavior (1 wk. time point only), cohort 2 focusing on isometric force and peripheral perfusion (1 wk. and 4 wk. time points), cohorts 3 and 4 focusing on isometric force and behavioral assessment (4 wk. time point only). Body and muscle weights were recorded and analyzed from all available cohorts. A final sample number for each assessment can be found in the figure legends.

### 2.6. Tissue collection

At 1 or 4 wks post-transplantation, gastrocnemius-soleus muscle complexes were collected from $CO_2$ asphyxiated animals. The muscles were weighed then frozen in pre-cooled isopentane. For the collection of the brains, animals were anesthetized with 200 mg/kg intraperitoneal sodium pentobarbital and then perfused transcardially with 4% paraformaldehyde in PBS. Brains were post-fixed overnight, and then transferred to 30% sucrose in PBS. Brains were sectioned with a cryostat into 40 μm-thick coronal sections. Sections were placed in tissue cryoprotectant (30% ethylene glycol, 25% glycerin, 45% PBS) in 24 well plates and stored at − 20 °C.

### 2.7. Skeletal muscle immunohistochemistry

Muscle complexes were divided at the midline along the axial plane, and embedded in OCT (Tissue-Tek; Fisher Scientific, Hanover Park, IL). Three transverse cryosections per sample (8 μm non-serial sections, each separated by a minimum of 40 μm) were cut for each histological assessment using a CM3050S cryostat (Lecia, Wezlar, Germany). Sections were placed on microscope slides (Superfrost; Fischer Scientific) and stored at − 80 °C before staining. Frozen skeletal muscle sections were fixed in ice-cold acetone for 10 min and blocked with PBS containing 5% bovine serum albumin (BSA) followed by 70 μg/ml AffiniPure anti-mouse Fab fragments diluted in 5% BSA (Jackson ImmunoResearch Laboratories, West Grove, PA) for 20 and 30 min, respectively. *To assess myofiber growth, satellite cell quantity, and myonuclear content*, tissue sections were co-stained with Pax7 (Developmental Studies Hybridoma Bank, University of Iowa, 1:2) and dystrophin antibodies (ab15277, 1:100) (Abcam). Both primary antibodies were diluted in 1% BSA, and were independently applied to the tissue sections at 4 °C overnight and 60 min at room temperature incubations, respectively. Fluorescein isothiocyanate (FITC)-labeled donkey anti-mouse (1:250), and tetramethyl rhodamine isothiocyanate (TRITC)-labeled goat anti-rabbit (1:100) secondary antibodies (Jackson ImmunoResearch Laboratories) were used to detect the Pax7 and dystrophin antibodies, respectively. A DAPI stain was added to the second to last wash step (1:20,000) (Sigma-Aldrich, St. Louis, MO) to allow for identification of nuclei. Sections were *co*-stained with rabbit polyclonal anti-Ki67 (1:100) (Abcam) and Pax7 to determine the average number of proliferating satellite cells as previously described [Huntsman et al., 2013]. Briefly, sections were incubated with Pax7 antibody at 4 °C overnight as described above. On the following day, sections were incubated with anti-KI67 for 1 h at room temperature. Finally, all sections were labeled with FITC anti-mouse (1:250) and Alexa Flour 633 anti-Rabbit (1 − 100) in 1% BSA for 1 h at room temperature. A DAPI stain was added to the second to last wash (1:20,000) to allow for identification of nuclei. *To assess skeletal muscle vascularity*, tissue sections were stained with a CD31 monocolonal antibody (eBioscience) for the detection of endothelial cells. Co-staining with a dystrophin monoclonal antibody (Sigma-Aldrich) was performed to assess tissue area necessary for evaluation of capillary density. Both primary antibodies were diluted to a concentration of 1:100 in PBS with 1% BSA, and were independently applied to the tissue sections and for an incubation period of 60 min at room temperature. FITC-labeled donkey anti-rat (1:250), and TRITC-labeled goat anti-mouse (1:100) secondary antibodies (Jackson ImmunoResearch Laboratories) were used to detect the CD31 and dystrophin antibodies, respectively. After each staining procedure, sections were mounted with Vectashield (Vector Laboratories).

### 2.8. Brain immunohistochemistry

For each protein (doublecortin, S100β, collagen IV), a one-in-six series of sections (240 μm) increments separating each section) through the dentate gyrus of the hippocampus were analyzed. *To assess immature neuron quantity (doublecortin$^+$; DCX$^+$)*, free-floating sections were washed in PBS and treated with a solution of 0.3% Triton-X and 6% normal donkey serum (NDS) in PBS (PBS-X plus 6% NDS) for 60 min [Perez et al., 2016]. Sections were then incubated in a PBS-X plus 6% NDS solution with primary antibody goat anti-DCX (1:1000, Santa Cruz Biotechnology) for 48 h at 4 °C. Sections were blocked with a solution of PBS-X plus 3% NDS for 20 min and incubated in biotinylated secondary antibody donkey anti-goat (1:200; Santa Cruz Biotechnology) in a solution of PBS-X plus 3% NDS for 90 min. Sections were then washed in a solution of 0.3% Triton-X in PBS and treated with the ABC system for 60 min (Vector Laboratories, Burlingame, CA), then stained with a DAB kit (Sigma-Aldrich). *For assessment of astrocyte quantity (S100$^+$)*, free-floating sections were washed in *Tris* buffered saline and incubated in 10% 20 × saline-sodium citrate buffer for 10 min at 37 °C. Sections were then treated with 0.3% hydrogen peroxide for 10 min; blocked with a solution of 10% normal goat serum (NGS) and 0.1% Triton-X in TBS (TBS-X plus 10% NGS). Free floating sections were incubated overnight in primary antibody rabbit anti-S100 (1:1000; Abcam) in TBS-X plus 3% NGS; washed in TBS, blocked in TBS-X plus 3% NGS and then incubated in biotinylated secondary antibody against rabbit made in goat (1:400, Vector Laboratories) in TBS-X; blocked; treated using the ABC system and stained as previously described for DCX. *For assessment of vascular density (collagen IV)*, free floating sections were washed in PBS, followed by distilled water at 37 °C [Clark et al., 2009]. Sections were then treated with pepsin (1 mg/ml) in 0.2 N HCl at 37 °C for 12 min for antigen retrieval, then washed in PBS for 15 min at 37 °C. Sections were then transferred to TBS, treated with 0.5% hydrogen

peroxide in TBS for 30 min, washed again in TBS, and then treated with 0.1% Triton-X and 3% goat serum in TBS. Sections were then incubated in primary antibody rabbit anti-collagen IV (1:300, Millipore) in TBS-X plus for 72 h. Following incubation, sections were washed in TBS, treated with TBS-X plus for 1 h, and then incubated in secondary antibody against rabbit made in goat at 1:500 in TBS-X plus for 90 min. Finally, sections were treated using the ABC system and stained as previously described for DCX. All sections were mounted on slides were then dehydrated in 70% and 50% alcohol for two minutes, 2 M PBS for two minutes and periodic acid for 7 min before staining methylene blue/azure II for 3 min. Sections were then dehydrated in alcohol and xylenes before mounting with Prolong gold anti-fade (Life Technologies) and cover-slipping.

### 2.9. Skeletal muscle image analysis

Tissue sections were visualized using an inverted fluorescent or brightfield light microscope (Zeiss, Thornwood, NY) and images were captured with a Zeiss AxioCam digital camera and Axiovision software (Zeiss). A combination of Adobe Photoshop (CS5 Extended) and ImageJ plug-ins and tools were used to analyze and quantitate all images acquired. A total of 20 digital images were acquired at 40 × magnification at random from each sample for evaluation of $Pax7^+$ satellite cells, $Pax7^+$ $Ki67^+$ cells, and fiber CSA. Assessments were made as previously described in detail [Huntsman et al., 2013]. An average of 500 fibers per sample were assessed for vascularization and fiber CSA as previously described in detail [Huntsman et al., 2013; Zou et al., 2015]. Briefly, to assess changes in skeletal muscle capillarization a total of 20 digital images acquired at 40 × magnification were captured at random from each sample. Images were acquired in separate color channels to allow for independent analysis of FITC (green) and TRITC (red) images. The CD31-FITC images were first analyzed for total number of transversely cut capillaries, as indicated by punctate, single cell staining, with the ImageJ template matching plug-in. Finally, the dystrophin-TRITC images were imported into Adobe Photoshop (CS5 Extended) where an average of 500 fibers per sample were manually circled using the magnetic lasso tool to decrease subjectivity and inter-assessor error by grabbing the positively stained pixels. Cross-sectional area measurements from each myofiber were recorded in the measurement log. Capillary density was calculated as total number of capillaries to area of tissue assessed.

### 2.10. Brain image analysis

For the evaluation of DCX-DAB positive cells, the entire granule layer (bilateral), from the one-in-six series stained for DCX-DAB, was imaged at 10 × (total 100 ×) magnification. All the cells in the series were counted except cells at the top of the section that were cut through the plane of the section to generate unbiased estimates following Clark et al. [2009]. For the evaluation of $S100^+$ cells in the molecular layer, a 1-in-12 series was imaged as described for DCX. For evaluation of brain vascularization, a grid overlay method was used in which the % collagen was determined by hand counting collagen intersections and dividing by total intersections minus white space [Rendeiro et al., 2015].

### 2.11. Functional measures (strength, peripheral perfusion, activity, cognitive performance)

All-limb grip strength was measured pre-treatment and 1 wk and 4 wks post-transplantation using an electronic Grip Strength Meter (Columbus Instruments, Columbus, OH). As an additional measure of strength, *maximal isometric force* was measured using a dual-mode lever system. Briefly, mice were fully anesthetized with 1–3% isoflurane gas before electrical stimulation of the sciatic nerve at 10 mA for 1.5 s (250 Hz). Muscle forces were collected using a servomotor and analog control unit (model 305C-LR, Aurora Scientific, Aurora, ON). Stimulation was repeated nine times with 5-s recovery periods, for a total of 10 measurements (trials). The values of maximal force output were normalized to muscle mass (g/mg). *Hindlimb perfusion* was assessed at three separate time points (1 wk. prior, and 1 wk. and 4 wks post-cell injection) using single-photon emission computed tomography – X-ray computed tomography (SPECT-CT). Mice were anesthetized with 1–3% isoflurane, and the left jugular vein was surgically exposed to facilitate intravascular injection of $^{99m}$Tc-tetrofosmin, a well-characterized blood perfusion radiotracer. Imaging was performed using a hybrid small animal SPECT-CT scanner (Inveon, Siemens Healthcare, Erlangen, Germany), with twenty 60 s SPECT and 360 CT projections captured per animal for a total of ~30 min of scanning time. All scans were analyzed using Inveon Research Workspace software (Siemens Healthcare, Erlangen, Germany). Briefly, complex irregular volumes of interest (VOIs) were generated from the CT images and applied on the co-registered SPECT images to calculate $^{99m}$Tc activities. These complex VOIs included only soft tissue (skeletal muscles) after the removal of bone structures during the image segmentation process. All mean values in both hindlimbs were normalized to 1 wk. time point and expressed as means and standard deviations of the mean. *Mean arterial BP* was measured in awake mice before, 1 and 4 wks after cell injection using tail-cuff method in restrained animals with CODA Surgical Monitor (Kent Scientific, United States) and expressed in mmHg. *Home cage activity* was assessed using TopScan video tracking software (Clever Sys Inc., VA) [Rendeiro et al., 2015]. Mice were placed in custom made home cages with video tracking from above. Daily distance traveled by the mice in their home cages was recorded over the course of four consecutive days. Average daily locomotion on days 3 and 4 after 2 days of habituation were chosen *a priori*, for analysis. All behavioral testing was completed during the dark phase of the light cycle to accommodate for enhanced activity during this time. Morris water maze (MWM), rotarod, and contextual fear conditioning (CFC) performance was assessed as previously described [Bhattacharya et al., 2015; Clark et al., 2012]. *MWM:* Mice were trained on a water maze with two trials per day for 5 days. Trials lasted either 60 s or after the mouse had reached the platform and remained there for 10 s. If a mouse did not reach the platform in 60 s, it was gently led to the platform by hand and remained there for 10 s. Mice were placed back in their cage and allowed to rest for 5 min between trials. One hour. after training on day 5, the platform was removed and mice were tested with a 60 s probe trial. The maze was a circular tank (70 cm diameter, 20 cm height), filled to a depth of 15 cm and white Crayola tempera paint was added to make the water opaque so the platform could not be seen. The platform consisted of a white plastic mesh circle (10 cm diameter) to match the color of the water, which was placed in the middle of one quadrant of the maze and submerged 0.5 cm below the surface of the water. Water temperature was maintained at 25 °C ( ± 1 °C). Extra-maze cues were placed around the room to facilitate learning. All trials were tracked using TopScan video software to evaluate path length to the platform (meters), latency to reach the platform (seconds) and swim speed (meters per second). For the probe trial, total number of crossings through the location where the platform previously resided, and total duration in the target quadrant were automatically recorded. *Rotarod:* After water maze, mice were tested for performance on a rotarod (AccuRotor Rota Rod Tall Unit, 63-cm fall height, 30- mm diameter rotating dowel; Accuscan, OH, USA). Mice were tested for performance on the rotarod for four consecutive trials per day for 2. The trial began with the dowel starting at 0 rpm and accelerated constantly at 60 rpm/min. The timer was automatically stopped when the mouse fell off the dowel and broke a photobeam at the base of the rotarod apparatus. *CFC*: Following rotarod, mice were tested for contextual fear conditioning. Mice were divided into groups, shock or control, across treatments. All mice were placed into a fear conditioning chamber for 180 s on day 1 and day 2. On day 1, mice in the shock group received 2 ft shocks (0.5 mA, 2 s duration) at 120 s and 150 s. Mice in the control group did not receive any foot shocks. On day 2, all mice were placed

into the chamber in the absence of any foot shock. The chamber consisted of a plastic cage (dim 32 × 28 × 30 cm L × W × H) with a wire grid bottom connected to a shock scrambler controlled by a digital timer (Med Associates, VT, USA). The animal's movement was tracked with a video camera mounted to the ceiling using TopScan video tracking software. Freezing was measured as the percent total number of seconds when the animal's center of mass did not register horizontal movement, as tracked by TopScan ( ± 1 mm).

### 2.12. Statistical analysis

*In vitro* cell data, muscle weight, fiber CSA, and capillary density were evaluated by two-way analysis of variance (ANOVA) (2 × 3 for *in vitro* data: No Strain and Strain × 11 kPa, 30 kPa, 110 kPa stiffness; 2 × 3 for *in vivo* data: Saline, mMSCs, mMSCs + Strain). Relative peak isometric force, Pax7$^+$ quantity, myonuclei:myofiber, DCX$^+$/S100$^+$ cell quantity, brain vascularization (% collagen IV), CFC duration freezing (shocked animals only) on day 2, and MWM probe trial data (duration in target quadrant, number of crossings through platform location) were evaluated by one-way ANOVA with treatment (Saline, mMSC, and mMSC + Strain) entered as the factor. Body weight, grip strength, relative isometric force (10 trials), mean arterial blood pressure, home cage activity (across 3 days), MWM acquisition (across 5 days), and rotarod assessment (2 days) were analyzed by 2-way ANOVA, with day as the repeated measures factor and treatment (Saline, mMSC, and mMSC + Strain) entered as the factor. Tukey's or least significant difference (LSD) *post hoc* analyses were used to compare the means between groups. Peripheral perfusion (1 *vs.* 4 wks) was analyzed with an independent *t*-test. All data were averaged and presented as means ± standard error, and were analyzed using SPSS (20.0, Chicago, IL) or Statistical Analyzing Software (9.2, Cary, NC). Data were log transformed if not normally distributed. Differences were considered significant at $p < 0.05$.

## 3. Results

### 3.1. In vitro mechanical strain influences mMSC gene expression and protein release

mMSCs (Sca-1$^+$CD45$^-$) were exposed to a single application of mechanical strain using an *in vitro* strategy previously described [Huntsman et al., 2013]. Conditioned media was evaluated using protein arrays and several factors were enhanced as a result of strain [Huntsman et al., 2013]. A full list of all factors released in response to strain (≥ 40% increase compared to media from non-strained cells) is shown in (Fig. 1A). EGF, endoglin, GM-CSF, Pref-1, resistin, angiogenin (Ang), chemokine (C-X-C motif) ligand 1 (CXCL1), leptin, and HGF protein content increased more than 50% in conditioned media 24 h following strain compared to non-strained media.

To determine the full potential for mechanical strain preconditioned mMSCs to sustain growth factor synthesis upon transplantation into aged muscle, non-strained and strained mMSCs were immediately placed on collagen-coated gels of varying stiffness (E = 11 kPa to mimic young healthy, E = 30 kPa to mimic aged, E = 110 kPa supra-physiological) and mMSC quantity and gene expression were evaluated 1 wk later (Fig. 1B). EGF, HGF and VEGF were chosen for evaluation based on their response to strain in the array and their ability to facilitate repair, satellite cell activation, and/or vascular adaptation [Anderson, 2016; Olfert et al., 2016]. mMSC Egf and Hgf mRNA increased in strained cells compared to non-strained cells (Egf strain x stiffness interaction, $F_{2,32}$ $p < 0.05$; Egf strain main effect, $F_{1,32} = 52.1$, $p < 0.001$; Egf stiffness main effect, $F_{2,32} = 6.23$, $p < 0.05$; Hgf strain main effect, $F_{1,32} = 21.28$, $p < 0.001$) (Fig. 1C–D). Vegfa mRNA was not altered in response to strain or stiffness (Fig. 1E).

### 3.2. Effect of preconditioned mMSCs on aged skeletal muscle

Aged mice received single, bilateral, intramuscular injections of saline, unstimulated mMSCs or mMSCs preconditioned with mechanical strain (mMSCs + Strain) (Fig. 2A). Body weight did not change as a result of treatment during the four wk. period following injection (Fig. 2B), yet muscle weight and mean fiber CSA were decreased in all treatment groups at 4 wks compared to 1 wk (muscle weight time main effect, $F_{1,73} = 14.891$, $p < 0.001$; fiber CSA time main effect, $F_{1,31} = 7.807$, $p < 0.05$) (Fig. 2C–D). A treatment main effect was observed for absolute force as assessed by grip strength ($F_{2,15} = 3.9$, $p < 0.05$) (Fig. 2E). Absolute force was significantly increased in mMSCs + Strain compared to Saline at 4 wks ($p < 0.05$) (Fig. 2E). Maximal isometric force of the plantar flexors was not altered at the four wk. time point (Fig. 2F), yet polynomial regression analysis revealed a treatment effect ($F_{2,45} = 3.4$, $p < 0.05$), with a significant upward shift in the force curve of mMSCs + Strain as compared to mMSCs ($p < 0.05$) following repeated contractions (Fig. 2G). Pax7$^+$ satellite cell quantity (normalized to total myonuclei) (Fig. 2H) and the percentage of Pax7$^+$ satellite cells co-expressing Ki67 were evaluated 1 wk post-transplantation (Fig. 2I). No significant differences were detected. The myonuclei:myofiber ratio also was not different between treatment groups at 1 wk (Fig. 2J).

### 3.3. mMSC transplantation increases blood perfusion in aged muscle

Vascularization (total number of CD31$^+$ vessels less than 5 μm) was not different between groups at 1 wk post-transplantation (Fig. 3A). Although the total number of CD31$^+$ vessels greater than 5 μm did not change significantly at this same time point, a trend toward an increase was observed in mMSCs + Strain at 1 wk post-transplantation compared to both control groups (Fig. 3B). No significant differences in arterial blood pressure were detected between treatment groups at 1 or 4 wks post-transplantation. The extent to which these observed changes could influence peripheral perfusion and resting flow in the hindlimb was assessed using SPECT-CT imaging (Fig. 3D). While no change was detected with injection of saline, a significant increase in peripheral perfusion was detected between 1 and 4 wks for the mMSCs (1.34-fold *vs.* 1 wk., $p < 0.05$) and mMSCs + Strain (1.53-fold *vs* 1 wk., $p < 0.05$) treatment groups (Fig. 3E).

### 3.4. Transplantation of preconditioned mMSCs increases hippocampal neurogenesis in aged mice

Studies were conducted to determine the extent to which mMSC transplantation could influence immature neuron formation (DCX$^+$ cell number) in the dentate gyrus of the hippocampus of aged recipient mice. The hippocampus from each animal was analyzed for DCX expression within the granular layer (Fig. 4A). A significant increase in DCX$^+$ cell quantity was observed when compared to both Saline and mMSCs ($F_{2,29} = 6.08$, $p < 0.01$ and $F_{2,29} = 5.20$, $p < 0.05$, respectively) (Fig. 4B). In addition, astrocyte quantity in the molecular layer of the dentate gyrus was altered by treatment (Fig. 4C–D). A significant increase in astrocyte number was detected in mMSCs + Strain compared to Saline ($F_{2,13} = 4.17$, $p < 0.05$) (Fig. 4D). Vascularization as assessed by collagen IV staining was not altered by treatment ($F_{3,13} = 0.67$, $p = 0.25$) (Fig. 4E).

### 3.5. Impact of preconditioned mMSCs on motor behavior and cognitive performance

Behavioral outcomes were measured during the four wk. period post-transplantation (Fig. 5A). No differences were detected in home cage activity (Fig. 5B). Mice learned the rotarod task as indicated by significant longer latency to fall on day 2 than day 1 ($F_{1,33} = 29.9$, $p < 0.001$), but no differences between groups were detected

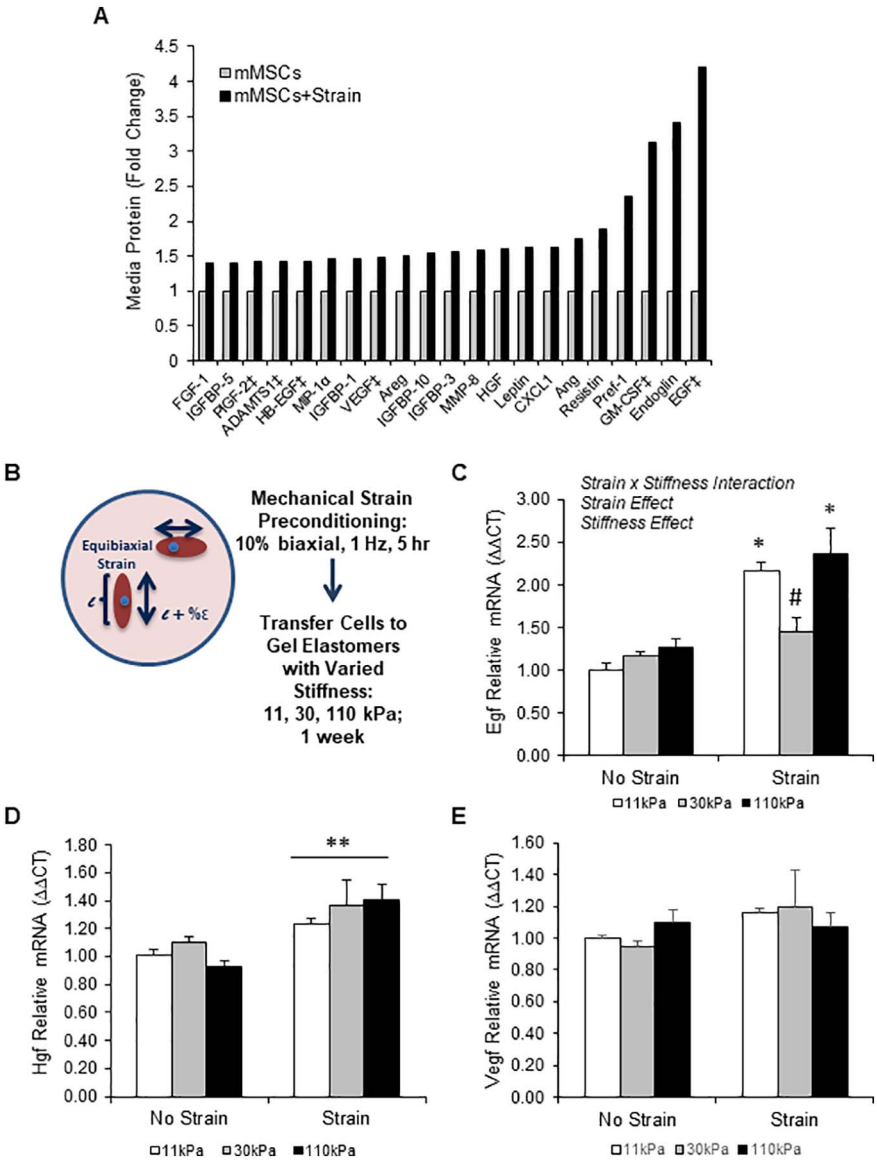


**Fig. 1.** *In vitro* mechanical strain increases mMSC protein release and enhances mMSC growth factor gene expression in a microenvironment that replicates aged skeletal muscle. **(A)** mMSCs were isolated from 5 wk. old mouse gastrocnemius-soleus muscle complexes and subjected to an acute bout of equibiaxial mechanical strain *in vitro* (laminin-coated Bioflex® membranes, 10% strain, 1 Hz, 5 h). Conditioned media ($n$ = 6/group, samples pooled) was evaluated for protein content at 24 h using a Proteome Profiler Antibody Array and the complete list of factors increased ≥1.40-fold post-strain is now reported. **(B)** Outline of *in vitro* mechanical strain preconditioning strategy prior to exposure to a microenvironment that replicates aged skeletal muscle. Following an acute bout of mechanical strain, mMSCs were transferred to gel elastomers coated with collagen and modified for stiffness (11, 30, 110 kPa) for 1 wk ($n$ = 5–6/group). **(C–E)** Effect of mechanical strain preconditioning on mMSC gene expression after exposure to collagen-coated gel elastomers with varying levels of stiffness. ‡ = data point previously reported in reference 5. $^{*}p < 0.05$ *vs.* all no strain groups and 30 kPa strain group, $^{\#}p < 0.05$ *vs.* 11 kPa no strain group, $^{**}p < 0.05$ strain main effect. Values are presented as means ± SE.

(Fig. 5C). To determine whether the increase in $DCX^{+}$ and $S100\beta^{+}$ expressing immature neurons translated to functional cognitive gains, spatial learning and memory and fear conditioning were assessed at 4 wks post-transplantation, as measured by MWM and CFC tasks. Mice displayed significant learning as indicated by decreased latency ($F_{4,132} = 15.9$, $p < 0.001$) and path length ($F_{4,132} = 17.2$, $p < 0.001$) to reach the platform across days, yet no significant differences between groups were detected for acquisition (data not shown). No differences were observed for number of crossings through the platform location during the probe trial. However, a trend was observed for an increase in preference for the target quadrant in mMSCs + Strain ($F_{2,32} = 2.8$, $p = 0.07$) during the one-hour recall probe trial (Fig. 5E). Mice significantly learned the CFC task as indicated by significant increase in freezing in the animals that were shocked on day 1 (average freezing was 2 s ± 1.2 SE) *versus* the unshocked controls (average freezing was 69.6 s ± 7.5 SE; $F_{1,15} = 54.4$, $p < 0.0001$), however, no significant differences were observed between treatment groups for CFC (data not shown).

## 4. Discussion

MSCs isolated from young muscle ($Sca\text{-}1^{+}CD45^{-}$) are primed to secrete beneficial growth, neurotrophic, and immunomodulatory factors following application of strain *in vitro* [Huntsman et al., 2013] (Fig. 1A). Thus, the primary purpose of this study was to determine the extent to which mMSCs preconditioned with mechanical strain could improve aged skeletal muscle structure and function. Our *in vivo* studies demonstrate that a single bilateral injection of preconditioned mMSCs ($4 \times 10^{4}$/limb) does not robustly alter progenitor cell activity, fiber growth, or maximal isometric force, suggesting that mMSC-based therapies may be limited in the ability to rejuvenate aged skeletal muscle. In contrast to the impact on muscle, intramuscular injection of preconditioned mMSCs increased the number of immature neurons and astrocytes in the dentate gyrus of the hippocampus, a finding that justifies further mechanistic evaluation of the link between muscle stem/stromal cells and neuroplasticity.

### 4.1. mMSCs secrete protein in response to mechanical strain

Due to the mechanical nature of the muscle microenvironment, and our previously published data demonstrating that mMSCs secrete regenerative growth factors such as EGF and HGF in response to mechanical strain [Huntsman et al., 2013; Fig. 1A], we hypothesized that this important biophysical cue could be implemented as an effective

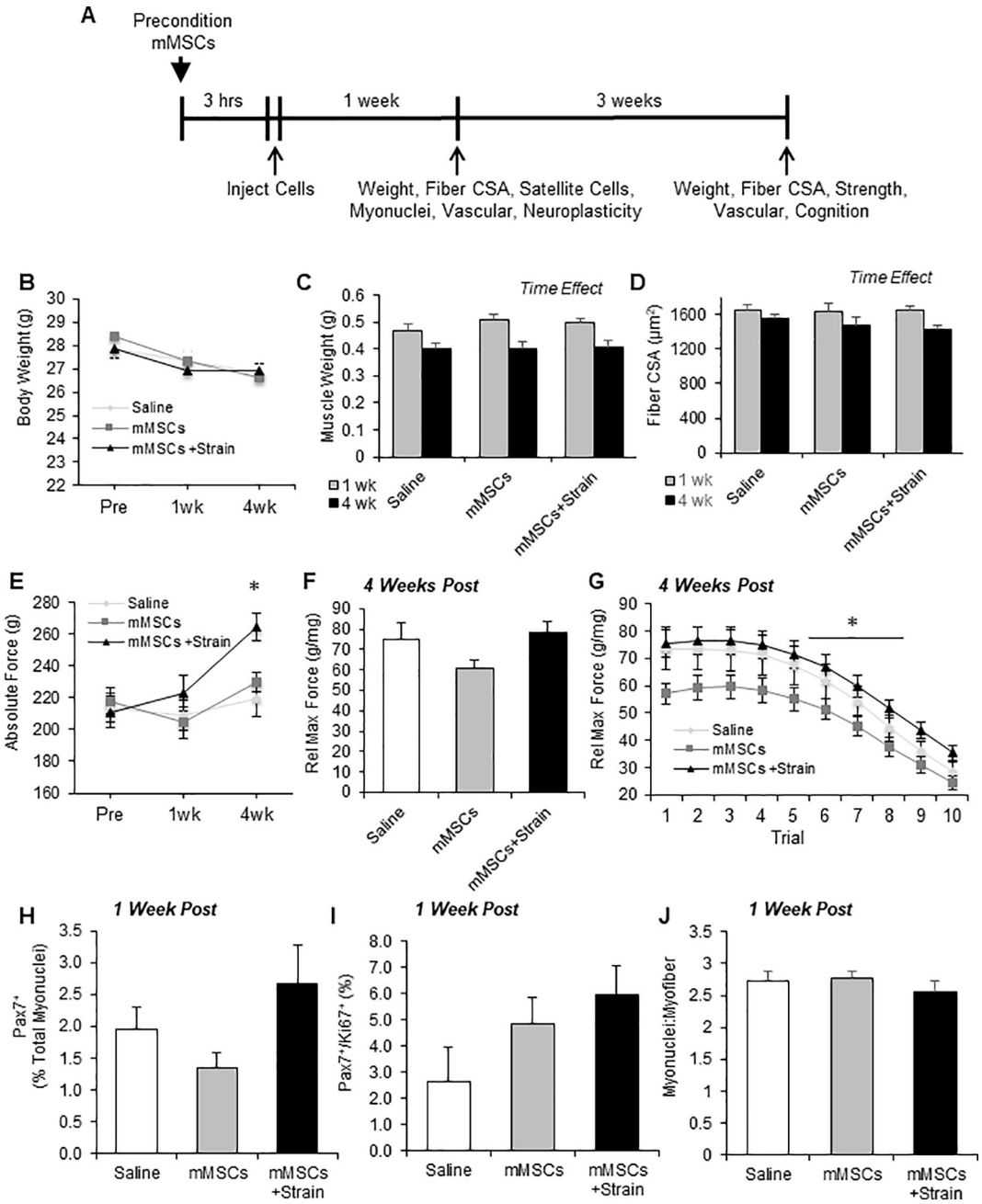


**Fig. 2.** Preconditioned mMSCs do not significantly alter skeletal muscle structure or function in aged mice. **(A)** Outline of *in vivo* study design. Aged mice received bilateral intramuscular injection of saline (Saline), unstimulated mMSCs (mMSCs), or mMSCs preconditioned with mechanical strain (mMSCs + Strain). **(B)** Body weight did not significantly change during the course of the experiment as a result of treatment ($n$ = 24–25/group, except saline, 4 wks $n$ = 15). **(C)** Muscle weight did not differ with treatment, but declined between 1 and 4 wks (1 wk.: $n$ = 8–9/group; 4 wks: $n$ = 15–17/group). **(D)** Fiber CSA did not differ with treatment, but declined between 1 and 4 wks (1 wk.: $n$ = 5/group; 4 wks: $n$ = 5–6) **(E)** Absolute force as assessed by dynamometry was increased in mMSCs + Strain compared to Saline at 4 wks (Pre: $n$ = 11–12/group; 1 wk.: $n$ = 11–12/group; 4 wks: $n$ = 6/group). **(F)** Maximal isometric force did not significantly change 4 wks post-transplantation ($n$ = 15–17/group). **(G)** A treatment main effect was detected for isometric force recorded during repeated stimulation ($n$ = 15–17/group). **(H–I)** Total satellite cell quantity and satellite cell proliferation was not altered 1 wk. post-transplantation ($n$ = 8–9/group). **(J)** Myonuclear content was not changed 1 wk. post-transplantation ($n$ = 5–6/group). *$p < 0.05$ treatment main effect. Values are presented as means ± SE.

preconditioning strategy to improve therapeutic outcomes associated with mMSC transplantation. The mechanical strain preconditioning method was verified in this study *in vitro* using PDMS gel elastomers that allow for adjustment of substrate (collagen) and stiffness to mimic the young, healthy and aged skeletal muscle microenvironments. Stiffness was chosen as the modulating variable due to the well-established relationship between stiffness and compromised tissue health [Reilly and Engler, 2010], and the fact that increased stiffness can result in inappropriate or unexpected stem cell behavior [Engler et al., 2006]. Similar to previous results [Huntsman et al., 2013], we found that mechanical strain enhanced mMSC Egf and Hgf mRNA expression for up to 1 wk compared to non-strained cells, and this pattern was maintained in a stiff (110 kPa), collagen-enriched environment (Fig. 1C–D). Although speculative, our data suggest that strain, rather than stiffness, is a primary regulator of the mMSC transcriptome.

### 4.2. Preconditioned mMSCs do not significantly improve structure or function of aged muscle

The success of the *in vitro* experiments encouraged us to evaluate the

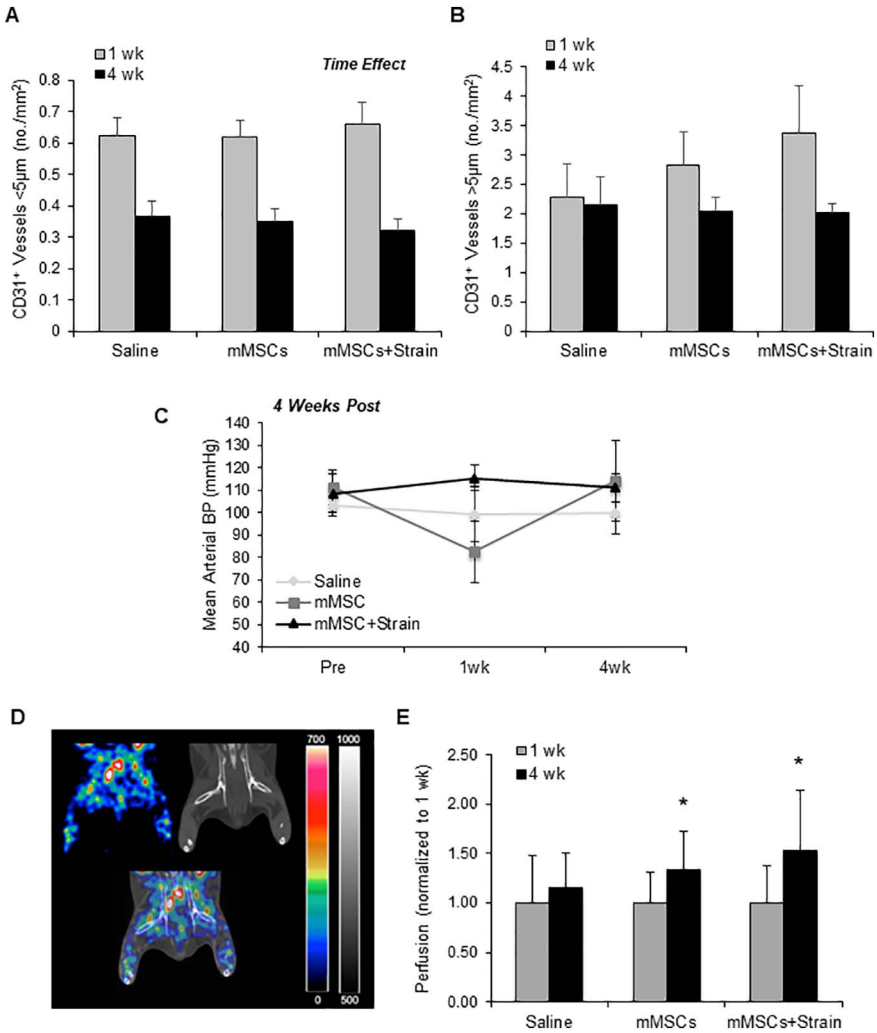


**Fig. 3.** mMSC transplantation improves blood perfusion in aged skeletal muscle. Aged mice received bilateral intramuscular injection of saline (Saline), unstimulated mMSCs (mMSCs) or mMSCs preconditioned with mechanical strain (mMSCs + Strain). **(A)** $CD31^+$ vessel density (< 5 μm) did not differ with treatment, but declined between 1 and 4 wks post-transplantation (1 wk.: $n$ = 8–9/group; 4 wks: $n$ = 5/group) **(B)** $CD31^+$ vessel density (> 5 μm) was not significantly increased as a result of treatment or time (1 wk.: $n$ = 8–9/group; 4 wks: $n$ = 5/group). **(C)** Arterial blood pressure was not changed at 1 or 4 wks post-transplantation (1 and 4 wks: $n$ = 5/group). **(D)** Representative SPECT, CT and fused SPECT-CT image of peripheral perfusion. Co-registered CT images were used to define irregular volumes-of-interests (VOIs) which were superimposed on SPECT images to measure perfusion radiotracer's uptake within the VOIs. Color maps represent count rate (for SPECT, nonlinear color scale) and arbitrary values of X-rays attenuation (for CT, grayscale). **(E)** Peripheral perfusion was quantified by measuring maximal uptake of $^{99m}$Tc-tetrofosmin from SPECT-CT images of each gastrocnemius muscle and expressed as right-to-left ratios (R/L). Perfusion is increased in both mMSCs and mMSCs + Strain groups at 4 wks relative to 1 wk. (1 and 4 wks: $n$ = 5/group). *$p$ < 0.05 *vs.* respective 1 wk. results. Values are presented as means ± SE.

extent to which preconditioned mMSCs could improve the structure and function of aged skeletal muscle. We chose to target aged animals only, and not young mice, due to the significant deficit in mMSC function previously observed in aged mice [Munroe et al., 2017]. No changes were observed in muscle weight or fiber size in aged mice at 1 or 4 wks following injection. A significant increase in strength using dynamometry was evident at 4 wks (Fig. 2E), but results from isometric testing did not verify this result (Fig. 2F–G). We previously reported small, but significant reductions in gastrocnemius-soleus complex weight (175–200 mg *vs.* 225–250 mg absolute weight) and strength in strain-matched aged mice compared to young [Munroe et al., 2017]. The lack of significant increase in muscle structure or function with a single injection in the current study suggests one of the following: 1) mechanical strain is not the biophysical cue required for mMSC-mediated promotion of adaptation following exercise training observed in young mice [Zou et al., 2015], 2) exogenously administered mMSCs cannot overcome significant fibrosis and declines in structure and function associated with advanced muscle aging (irreversible damage), and/or 3) higher doses of preconditioned mMSCs or multiple rounds of injection are required to overcome barriers and effectively rejuvenate aged muscle. The significant reductions in muscle weight, fiber CSA, and vascular structure observed between weeks 1 and 4 were unexpected (Fig. 2C–D, Fig. 3A–B), and likely reflect variability among the two cohorts of mice studied rather than the process of natural aging. Regardless, a treatment effect was not noted at either time point.

### 4.3. Preconditioned mMSCs do not stimulate satellite cell proliferation or expansion as assessed 1 wk post-injection

We have previously reported a beneficial effect of mMSCs on satellite cell quantity within 24 h following acute exercise [Valero et al., 2012], and satellite cells rapidly respond to an exercise stimulus and return to baseline levels by 1 wk [Lueders et al., 2011]. In the current study, satellite cells appeared to positively respond to mMSC injection (Fig. 2H–I), yet the results were not significant at the relatively late time point of 1 wk post-injection. A more extensive follow up study will be necessary to determine the full extent to which preconditioned mMSCs can acutely stimulate satellite cell dynamics in aged muscle in the absence of injury.

### 4.4. mMSC transplantation improves peripheral perfusion in aged muscle

In contrast to the results for myofiber structure and strength, a single injection of mMSCs positively influenced vascular structure and function in aged muscle. Compared to prior data collected for young mice (3 month old) [Huntsman et al., 2013], baseline numbers of capillaries ($CD31^+$ vessels < 5 μm) and larger vessels ($CD31^+$ vessels > 5 μm with visible lumen) were reduced in aged mice in the current study. Consistent with previous findings in young mice following eccentric exercise [Huntsman et al., 2013], injection of preconditioned mMSCs in aged muscle did not contribute to angiogenesis (Fig. 3A), but did tend to influence capacity for vessel growth at 1 wk post-injection (number of vessels > 5 μm) (Fig. 3B). Peripheral

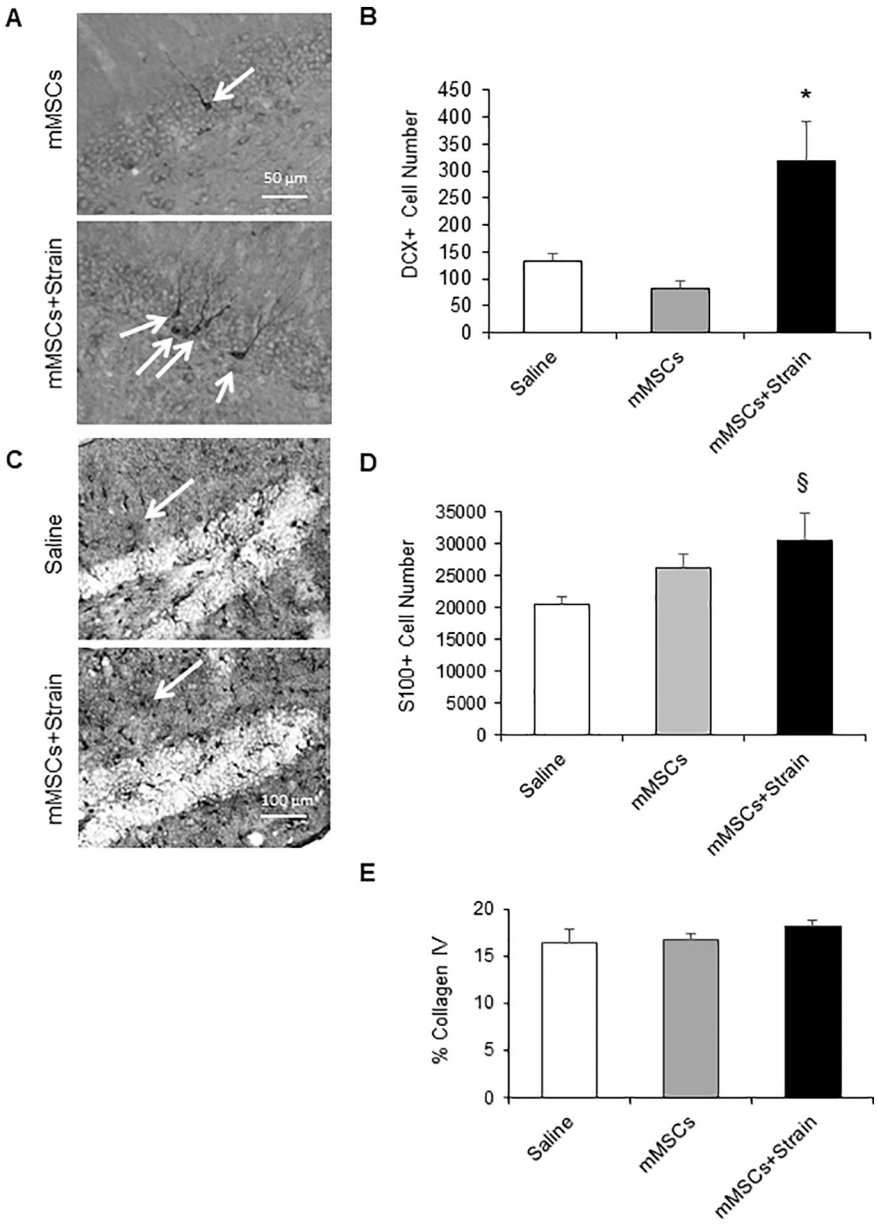


**Fig. 4.** Intramuscular transplantation of preconditioned mMSCs positively impacts immature neuron formation in the distal hippocampus of aged mice. Aged mice received bilateral intramuscular injection of saline (Saline), unstimulated mMSCs (mMSCs) or mMSCs preconditioned with mechanical strain (mMSCs + Strain). **(A)** Representative images of the dentate gyrus of the hippocampus stained for doublecortin (DCX) from a 24 mo old animal following transplantation. Scale bar = 50 µm. **(B)** $DCX^+$ cell number was significantly increased in the granular layer of the dentate gyrus 1 wk. following transplantation of preconditioned mMSCs compared to controls (Saline: $n = 11$; mMSC: $n = 5$; mMSC + Strain: $n = 10$). **(C)** Representative images of the molecular layer of the dentate gyrus stained for $S100^+$ astrocytes. Scale bar = 100 µm. **(D)** Astrocyte quantity was significantly increased in the molecular layer of the dentate gyrus 1 wk. following transplantation of preconditioned mMSCs compared to Saline ($n = 5$–6/group). **(E)** Vascularization of the dentate gyrus of the hippocampus as assessed by collagen IV staining was not altered 1 wk. post-transplantation ($n = 5$–6/group). $^*p < 0.05$ *vs.* all other groups, $^§p < 0.05$ *vs.* Saline. Values are presented as means ± SE.

perfusion as assessed by SPECT-CT was increased at 4 wks compared to 1 wk following injection of mMSCs or preconditioned mMSCs (Fig. 3E). We speculate that mMSC-mediated secretion of pro-arteriogenic factors (endoglin, GM-CSF, resistin, Ang, CXCL1, leptin, HGF, and VEGF) [Huntsman et al., 2013; Fig. 1A] initiated an early vascular remodeling event that then positively impacted tone at the later time point. This adaptation may be appropriate given the ability for perivascular stem/stromal cells to interact with endothelial cells and directly regulate vessel structure and function. Overall, the current results suggest that mMSCs improve peripheral vessel remodeling and function in aged skeletal muscle.

### *4.5. Preconditioned mMSCs increase new neuron and astrocyte quantity in the hippocampus of aged mice*

Paracrine factor secretion by skeletal muscle has been recently explored as a potential mechanism underlying the positive effects of physical exercise on brain plasticity, neurogenesis and cognitive function [Fabel et al., 2003; Moon et al., 2016; Trejo et al., 2001; Wrann et al., 2013]. Serum IGF and VEGF may play a role, as the peripheral blockade of these abolished the running-induced enhancement of hippocampal neurogenesis [Fabel et al., 2003; Trejo et al., 2001]. Furthermore, irisin and cathepsin B have been implicated as muscle secretory proteins with capacity for improving hippocampal neurogenesis and spatial memory in mice following exercise [Moon et al., 2016; Wrann et al., 2013]. The extent to which muscle-resident stromal cells contribute to the systemic factor-mediated changes in hippocampal plasticity has not been explored. The number of newborn immature neurons was typical for aged mice [Jinno, 2011; Marlatt et al., 2012; Wu et al., 2008], and injection of preconditioned mMSCs elicited a 2- to 3-fold increase in the total number of $DCX^+$ cells in the dentate gyrus of the hippocampus of aged mice compared to control groups (Fig. 4A–B). This was accompanied by a significant increase in astrocyte number in comparison with saline-treated mice (Fig. 4C–D). The rise in $DCX^+$-expressing neurons is similar to what has been reported as result of physical exercise interventions (typically increases ranging from 2- to 5-fold) [Garrett et al., 2012; Gebara et al., 2013; Wu et al., 2008]. It is tempting to speculate that the increase in peripheral perfusion underlies beneficial adaptations in brain stem cell behavior observed. However, perfusion was equally enhanced with injection of unstrained and

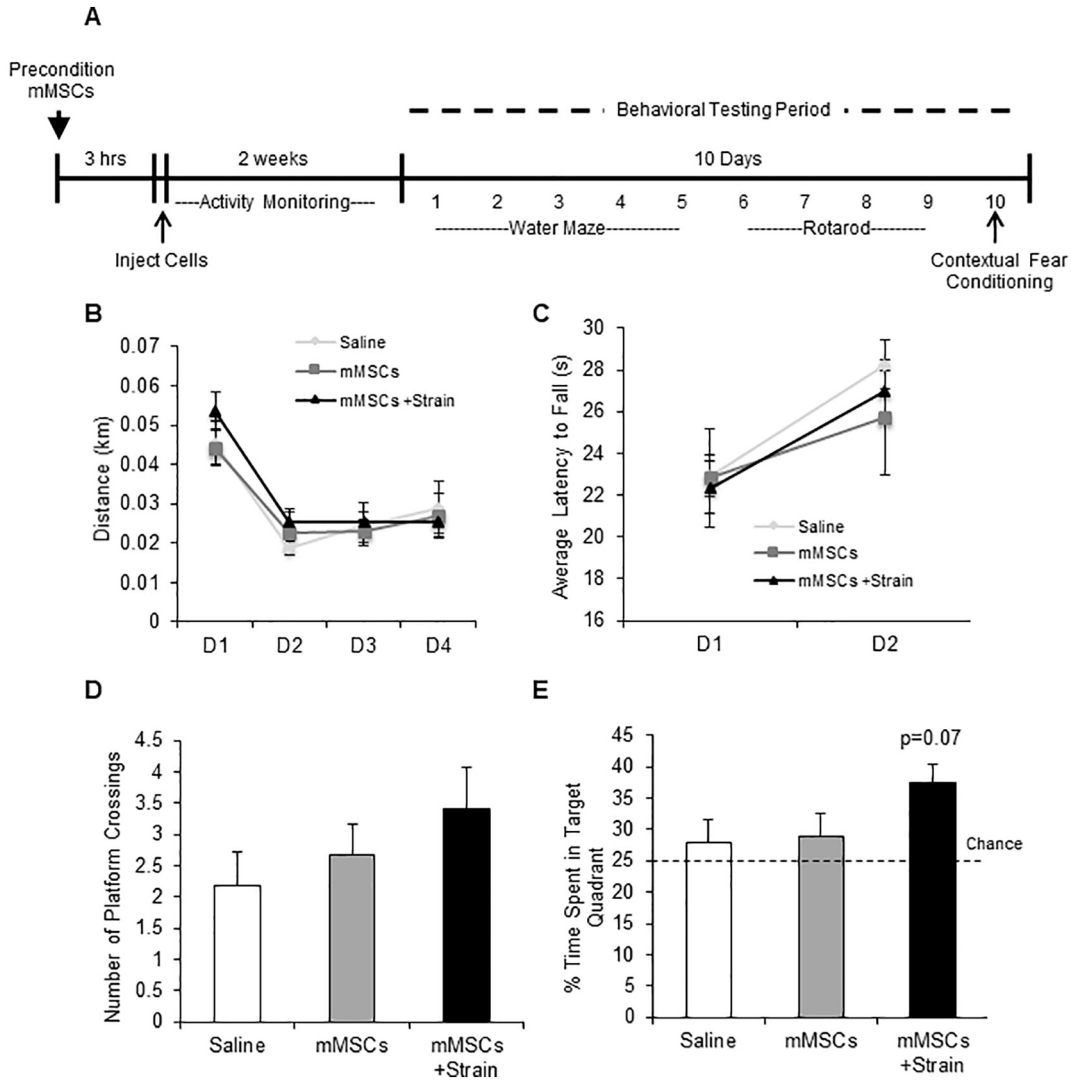


**Fig. 5.** Impact of preconditioned mMSCs on activity, balance and spatial learning. **(A)** Outline of behavioral analyses. **(B)** Daily activity was monitored over the course of 4 days using TopScan video tracking software. No significant differences were observed between treatment groups. **(C)** No significant differences were observed for rotarod performance between treatment groups. **(D–E)** Cognitive function was examined by Morris water maze. No differences were observed for number of crossings through the platform location during the probe trial. However, a trend toward an increase in duration spent in the target quadrant was noted ($p = 0.07$). $n = 11–12$/group for all experiments. Values are presented as means ± SE.

strained mMSCs, whereas neurogenesis was only significant with injection of strained mMSCs. Thus, a combination of enhanced perfusion and redistribution of select neurotrophic factors derived from mMSCs may be required to promote neuroplasticity in the aged brain. Further investigation of mMSC factor release using high throughput technologies will be necessary to identify the full repertoire of neurogenic stimuli released from mMSCs in response to mechanical strain.

### 4.6. Preconditioned mMSCs positively impact spatial learning in aged mice

In the course of adult hippocampal neurogenesis, most regulation takes place during the phase of DCX expression (3 days to 3 wks) [Brown et al., 2003; Plumpe et al., 2006], during which post mitotic newborn immature neurons undergo morphological changes, such as neurite extension and synaptogenesis until they reach full maturity (when they stop expressing DCX). Notably, DCX-expressing newborn neurons have unique properties, such as increased excitability [Karl et al., 2005] and lower thresholds for activation and induction of long-term potentiation (LTP) [Cheng et al., 2011]. $DCX^+$ cells must be at least 3 to 4 wks old before they can make a significant contribution to spatial learning [Gu et al., 2012]. In line with this, we observed a trend toward an improvement in hippocampal-dependent spatial memory task 4 wks post-treatment with preconditioned mMSCs (Fig. 5E).

One limitation to the current study is that the survivability of mMSCs in muscle post-transplantation could not be established. We attempted to identify cells using *in situ* hybridization for the Y chromosome (male cells injected into female mice). We were able to confirm the presence of the cells, but permeability of the nuclear membrane was incomplete in some cells and quantitation was unreliable. Based on subjective analysis, the quantity did not appear to be different between mMSCs and mMSCs + Strain, but we cannot rule out the possibility that strain increased the survival of the mMSCs post-transplantation, accounting for the enhancement in neurogenesis.

## 5. Conclusion

In conclusion, this study is the first to demonstrate that 1) mechanical strain can facilitate mMSC release of paracrine factors, and select growth factor gene expression is sustained in a simulated aged microenvironment, and 2) a single, intramuscular injection of mMSCs preconditioned with mechanical strain does not significantly impact aged skeletal muscle, but can positively impact survival of newborn neurons in the hippocampus, potentially resulting in a beneficial impact on spatial memory. Our results highlight an important link between

muscle-resident stem/stromal cells and neuroplasticity, justifying future studies to examine the mechanism of communication between these important regenerative cell types.

## Conflicts of interest

Abbott Nutrition contributed research funding necessary to complete this work (Abbott CNLM ZA68 to MDB and ZB32 to JSR).

## Acknowledgements

We would like to thank Tushar Bhattacharya, Nicole Zachweija, Eli Khazoum, and Kelly Ryan for their assistance in data collection and analysis. We would also like to thank Drs. Koyal Garg (Saint Louis University), Dr. Jie Chen (UIUC), and Nidhi Khanna (UIUC) for scientific contributions and insight necessary for completion of this study.

## Funding

HDH was funded at UIUC from National Science Foundation (NSF) Grant 0965918 IGERT: Training the Next Generation of Researchers in Cellular and Molecular Mechanics and BioNanotechnology. This work was supported by grants from the Ellison Medical Foundation (AG-NS-0547-09) (to MDB) and Abbott Nutrition through the Center for Nutrition, Learning, and Memory (CNLM) at the University of Illinois (CNLM ZA68 to MDB and ZB32 to JSR).

## Author contributions

HDH: Conception and design, collection of data, data analysis and interpretation, manuscript writing, final approval.

CR: Collection of data, data analysis and interpretation, manuscript writing, final approval.

JRM: Collection of data, data analysis and interpretation, manuscript writing, final approval.

YP: Collection of data, data analysis and interpretation, final approval.

AC: Collection of data, final approval.

MD: Collection of data, final approval.

EK: Collection of data, final approval.

SD: Collection of data, final approval.

ITD: Collection of data, final approval.

RK: Conception and design, final approval.

TJ: Collection of data, final approval.

LWD: Collection of data, final approval.

JR: Conception and design, data analysis and interpretation, final approval, financial support.

MDB: Conception and design, data analysis and interpretation, manuscript writing, final approval, financial support.

## References

Anderson, J.E., 2016. Hepatocyte growth factor and satellite cell activation. Adv. Exp. Med. Biol. 900, 1–25.

Augello, A., Kurth, T.B., De Bari, C., 2010. Mesenchymal stem cells: a perspective from in vitro cultures to in vivo migration and niches. Eur. Cell Mater. 20, 121–133.

Bhattacharya, T.K., Pence, B.D., Ossyra, J.M., Petr, G., Martin, S.A., Wang, L., Rubakhin, S.S., Sweedler, J.V., McCusker, R.H., Kelley, K.W., Rhodes, J.S., Johnson, R.W., Woods, J.A., 2015. Exercise but not (−)-epigallocatechin-3 gallate or beta-alanine enhances physical fitness, brain plasticity, and behavioral performance in mice. Physiol. Behav. 145, 29–37.

Brown, J.P., Couillard-Despres, S., Cooper-Kuhn, C.M., Winkler, J., Aigner, L., Kuhn, H.G., 2003. Transient expression of doublecortin during adult neurogenesis. J. Comp. Neurol. 467, 1–10.

Carnio, S., LoVerso, F., Baraibar, M.A., Longa, E., Khan, M.M., Maffei, M., Reischl, M., Canepari, M., Loefler, S., Kern, H., Blaauw, B., Friquet, B., Bottinelli, R., Rudolf, R., Sandri, M., 2014. Autophagy impairment in muscle induces neuromuscular junction degeneration and precocious aging. Cell Rep. 8, 1509–1521.

Cheng, X., Li, Y., Huang, Y., Geng, X., Feng, G., Xiong, Z.Q., 2011. Pulse labeling and long-term tracing of newborn neurons in the adult subgranular zone. Cell Res. 21, 338–349.

Clark, P.J., Brzezinska, W.J., Puchalski, E.K., Krone, D.A., Rhodes, J.S., 2009. Functional analysis of neurovascular adaptations to exercise in the dentate gyrus of young adult mice associated with cognitive gain. Hippocampus 19, 937–950.

Clark, P.J., Bhattacharya, T.K., Miller, D.S., Kohman, R.A., DeYoung, E.K., Rhodes, J.S., 2012. New neurons generated from running are broadly recruited into neuronal activation associated with three different hippocampus-involved tasks. Hippocampus 22, 1860–1867.

Conboy, I.M., Conboy, M.J., Smythe, G.M., Rando, T.A., 2003. Notch-mediated restoration of regenerative potential to aged muscle. Science 302, 1575–1577.

Engler, A.J., Sen, S., Sweeney, H.L., Discher, D.E., 2006. Matrix elasticity directs stem cell lineage specification. Cell 126, 677–689.

Fabel, K., Fabel, K., Tam, B., Kaufer, D., Baiker, A., Simmons, N., Kuo, C.J., Palmer, T.D., 2003. VEGF is necessary for exercise-induced adult hippocampal neurogenesis. Eur. J. Neurosci. 18, 2803–2812.

Fan, J., Kou, X., Jia, S., Yang, X., Yang, Y., Chen, N., 2016. Autophagy as a potential target for sarcopenia. J. Cell. Physiol. 231, 1450–1459.

Garrett, L., Lie, D.C., Hrabe de Angelis, M., Wurst, W., Holter, S.M., 2012. Voluntary wheel running in mice increases the rate of neurogenesis without affecting anxiety-related behaviour in single tests. BMC Neurosci. 13, 61.

Gebara, E., Sultan, S., Kocher-Braissant, J., Toni, N., 2013. Adult hippocampal neurogenesis inversely correlates with microglia in conditions of voluntary running and aging. Front. Neurosci. 7, 145.

Gu, Y., Arruda-Carvalho, M., Wang, J., Janoschka, S.R., Josselyn, S.A., Frankland, P.W., Ge, S., 2012. Optical controlling reveals time-dependent roles for adult-born dentate granule cells. Nat. Neurosci. 15, 1700–1706.

Huntsman, H.D., Zachwieja, N., Zou, K., Ripchik, P., Valero, M.C., De Lisio, M., Boppart, M.D., 2013. Mesenchymal stem cells contribute to vascular growth in skeletal muscle in response to eccentric exercise. Am. J. Physiol. Heart Circ. Physiol. 304, H72–81.

Jinno, S., 2011. Decline in adult neurogenesis during aging follows a topographic pattern in the mouse hippocampus. J. Comp. Neurol. 519, 451–466.

Karl, C., Couillard-Despres, S., Prang, P., Munding, M., Kilb, W., Brigadski, T., Plotz, S., Mages, W., Luhmann, H., Winkler, J., Bogdahn, U., Aigner, L., 2005. Neuronal precursor-specific activity of a human doublecortin regulatory sequence. J. Neurochem. 92, 264–282.

Katsanos, C.S., Kobayashi, H., Sheffield-Moore, M., Aarsland, A., Wolfe, R.R., 2006. A high proportion of leucine is required for optimal stimulation of the rate of muscle protein synthesis by essential amino acids in the elderly. Am. J. Physiol. Endocrinol. Metab. 291, E381–7.

Kumar, V., Selby, A., Rankin, D., Patel, R., Atherton, P., Hildebrandt, W., Williams, J., Smith, K., Seynnes, O., Hiscock, N., Rennie, M.J., 2009. Age-related differences in the dose-response relationship of muscle protein synthesis to resistance exercise in young and old men. J. Physiol. 587, 211–217.

Lee, J.D., Fry, C.S., Mula, J., Kirby, T.J., Jackson, J.R., Liu, F., Yang, L., Dupont-Versteegden, E.E., McCarthy, J.J., Peterson, C.A., 2016. Aged muscle demonstrates fiber-type adaptations in response to mechanical overload, in the absence of myofiber hypertrophy, independent of satellite cell abundance. J. Gerontol. A Biol. Sci. Med. Sci. 71, 461–467.

Lueders, T.N., Zou, K., Huntsman, H.D., Meador, B., Mahmassani, Z., Abel, M., Valero, M.C., Huey, K.A., Boppart, M.D., 2011. Am. J. Phys. Cell Phys. 301, C938–46.

Marlatt, M.W., Potter, M.C., Lucassen, P.J., van Praag, H., 2012. Running throughout middle-age improves memory function, hippocampal neurogenesis, and BDNF levels in female C57BL/6J mice. Dev. Neurobiol. 72, 943–952.

Meirelles Lda, S., Fontes, A.M., Covas, D.T., Caplan, A.I., 2009. Mechanisms involved in the therapeutic properties of mesenchymal stem cells. Cytokine Growth Factor Rev. 20, 419–427.

Moon, H.Y., Becke, A., Berron, D., Becker, B., Sah, N., Benoni, G., Janke, E., Lubejko, S.T., Greig, N.H., Mattison, J.A., Duzel, E., van Praag, H., 2016. Cell Metab. 24, 332–340.

Munroe, M., Pincu, Y., Merritt, J., Cobert, A., Brander, R., Jensen, T., Rhodes, J., Boppart, M.D., 2017. Impact of β-hydroxy β-methylbutyrate (HMB) on age-related functional deficits in mice. Exp. Gerontol. 87, 57–66 (Pt A).

Murray, I.R., Corselli, M., Petrigliano, F.A., Soo, C., Peault, B., 2014. Natural history of mesenchymal stem cells, from vessel walls to culture vessels. Cell. Mol. Life Sci. 71, 1353–1374.

Olfert, I.M., Baum, O., Hellsten, Y., Egginton, S., 2016. Advances and challenges in skeletal muscle angiogenesis. Am. J. Physiol. Heart Circ. Physiol. 310, H326–36.

Perez, S.D., Du, K., Rendeiro, C., Wang, L., Wu, Q., Rubakhin, S.S., Vazhappilly, R., Baxter, J.H., Sweedler, J.V., Rhodes, J.S., 2016. A unique combination of micronutrients rejuvenates cognitive performance in aged mice. Behav. Brain Res. 320, 97–112.

Plumpe, T., Ehninger, D., Steiner, B., Klempin, F., Jessberger, S., Brandt, M., Romer, B., Rodriguez, G.R., Kronenberg, G., Kempermann, G., 2006. Variability of doublecortin-associated dendrite maturation in adult hippocampal neurogenesis is independent of the regulation of precursor cell proliferation. BMC Neurosci. 7, 77.

Ranganath, S.H., Levy, O., Inamdar, M.S., Karp, J.M., 2012. Harnessing the mesenchymal stem cell secretome for the treatment of cardiovascular disease. Cell Stem Cell 10, 244–258.

Reilly, G.C., Engler, A.J., 2010. Intrinsic extracellular matrix properties regulate stem cell differentiation. J. Biomech. 43, 55–62.

Rendeiro, C., Masnik, A.M., Mun, J.G., Du, K., Clark, D., Dilger, R.N., Dilger, A.C., Rhodes, J.S., 2015. Fructose decreases physical activity and increases body fat without affecting hippocampal neurogenesis and learning relative to an isocaloric glucose diet. Sci. Rep. 5, 9589.

Trejo, J.L., Carro, E., Torres-Aleman, I., 2001. Circulating insulin-like growth factor I mediates exercise-induced increases in the number of new neurons in the adult hippocampus. J. Neurosci. 21, 1628–1634.

Valero, M.C., Huntsman, H.D., Liu, J., Zou, K., Boppart, M.D., 2012. Eccentric exercise facilitates mesenchymal stem cell appearance in skeletal muscle. PLoS One 7, e29760.
Wrann, C.D., White, J.P., Salogiannnis, J., Laznik-Bogoslavski, D., Wu, J., Ma, D., Lin, J.D., Greenberg, M.E., Spiegelman, B.M., et al., 2013. Exercise induces hippocampal BDNF through a PGC-1α/FNDC5 pathway. Cell Metab. 18, 649–659.
Wu, C.W., Chang, Y.T., Yu, L., Chen, H.I., Jen, C.J., Wu, S.Y., Lo, C.P., Kuo, Y.M., 2008. Exercise enhances the proliferation of neural stem cells and neurite growth and survival of neuronal progenitor cells in dentate gyrus of middle-aged mice. J. Appl. Physiol. 105, 1585–1594.
Zou, K., Huntsman, H.D., Carmen Valero, M., Adams, J., Skelton, J., De Lisio, M., Jensen, T., Boppart, M.D., 2015. Mesenchymal stem cells regulate the adaptive response to eccentric exercise. Med. Sci. Sports Exerc. 47, 315–325.